Thermophonon flux in double-cavity optomechanics

Yu Wu,[1] Wenjie Nie,[1,*] Guoyao Li,[1] Aixi Chen,[2,†] and Yueheng Lan[3,‡]
[1]*Department of Applied Physics, East China Jiaotong University, Nanchang 330013, China*
[2]*Department of Physics, Zhejiang Sci-Tech University, Hangzhou 310018, China*
[3]*Department of Physics, Beijing University of Posts and Telecommunications, Beijing 100876, China*

(Received 26 September 2020; accepted 13 April 2021; published 29 April 2021)

We propose theoretically an optomechanical system with double cavities to explore the thermophonon transport from the thermal bath of the mechanical oscillator to the coupled system. We find that the direction and magnitude of thermophonon flux in the system can be controlled flexibly by coupling an active cavity with gain to the driven cavity. In particular, the injected squeezing vacuum can reverse the nonequilibrium characteristics of the system and change the thermophonon flux from positive to negative. We also investigate in detail the influence of the driving power and the photon tunneling strength on the flux, which can widen the energy transfer channel of the system. The results obtained here have a potential application in the thermal noise energy harvesting and rectification by the optomechanical setup.

DOI: 10.1103/PhysRevA.103.043521

I. INTRODUCTION

It is well known that energy transfers generally from a hot source to a cold one and its realization can resort in the coupling between the mechanical oscillators being immersed into different thermal baths, which helps one identify the general features of energy transports in nonequilibrium physics [1–4]. For example, it is found that classical heat transports in a dissipative open system with two coupled oscillators can be regulated by changing the dissipative strengths between the oscillators and baths as well as the temperature of the thermal environment [5]. Further, the nonlinearity plays an important role in controlling the steady-state heat flux across an overdamped anharmonic junction with arbitrary temperature bias [6]. Moreover, the rapid development of nanotechnology promotes the study of quantum heat transfer and its dynamical regulation in nanoscale systems, such as a nanojunction connecting two thermal baths [7–9], semiconductor nanowires [10], silicon membranes [11], molecular chains [12–14], and so on. In particular, the identification of the nonequilibrium quantum transport through the low-dimensional systems guides one to design thermal-based nanoscale devices, such as thermal diodes [15,16] and thermal rectifiers [17–19], and therefore has much application in phononics [4].

In recent years, we have also witnessed the rapid development of cavity optomechanical systems with micro- or nanoscale movable parts, which aim to realize the coupling between light and mechanical motion modes and further explore the quantum effect in macroscopic motions, i.e., ground-state cooling [20–26], quantum entanglement [27–29], mechanical squeezing [30,31], optomechanically induced transparency (OMIT) [32–35], and so on. In general, the optomechanical system is always treated as an open quantum system and the driven cavity field plays the role of the quantum oscillator coupled to a zero-temperature or vacuum environment. As a result, the pumping cooling of the mechanical motion in optomechanical systems benefits from the transfer of mechanical energy from a thermal bath to vacuum environment through photon dissipation [36]. It is noted that the cavity optomechanical systems can be used as a unique platform to explore the design of the quantum thermal rectifier by manipulating the flow of thermal noise [37]. Other thermodynamic applications of optomechanical systems, i.e., proposals for the optomechanical quantum heat engine [38–43] and nonreciprocal optomechanical heat transport [44,45], have been investigated in detail, which helps demonstrate the all-optical control of the quantum thermodynamical effect in small systems and the significant role of the optomechanical coupling of the optical and mechanical modes.

The context of this work highlights a proposed double-cavity optomechanical system with gain and loss, for exploring the characteristics of thermophonon transport in a coupled oscillator system with thermal and vacuum dissipation sources. The complicated proposal with gain and loss optical cavities has been extensively designed to construct parity-time ($\mathcal{PT}$)-symmetric optomechanical systems, where many interesting physical behaviors, such as mechanical $\mathcal{PT}$ symmetry [46,47], ultralow threshold chaos [48], phonon laser [49,50], and distinguishing photon blockade [51], have been investigated in detail. Moreover, the light transmission patterns in the optomechanical systems with gain can be changed by simply adjusting the coupling strength between the gain and loss optical cavities as well as the gain-to-loss ratio [35,52,53]. This benefits from the gain photons tunneling between the optical cavities, which also regulates the

*niewenjiezhu@sina.cn
†aixichen@zstu.edu.cn
‡lanyh@bupt.edu.cn

energy transfer between the system and its dissipative sources. Therefore, it will be interesting and important to study the thermal noise energy harvesting and rectification in optomechanical systems with gain environment. In this work, the main motivation is to derive the general expressions of the steady-state thermophonon flux in coupled oscillator systems with gain by using the cumulant generating function (CGF) approach [5]. Correspondingly, we investigate the thermal noise flux between the mechanical oscillator and double-cavity system and examine the dependence of phonon flux on the adjacent cavity and optomechanical coupling between the cavity field and the mechanical oscillator. In particular, this study aims to explore the change of the direction of the thermophonon flux when the squeezed vacuum field is injected into the passive optical cavity, which can be used to change optically nonequilibrium characteristics of the system. Furthermore, an attempt is made to demonstrate the manipulation of the thermophonon flux when the three-mode optomechanical system works in the $\mathcal{PT}$-symmetric regime. With such, the direction of thermophonon flux in the optomechanical system is found to be controlled by changing the photon-tunneling coupling between the gain and loss optical cavities and the gain of the adjacent cavity. The influences of the laser power and the decay rate of the adjacent cavity on the characteristics of the thermophonon flux in the system are discussed in detail. The results attained here are helpful for the thermal noise energy harvesting and rectification in optomechanical systems by means of all-optical regulation.

The rest of the paper is organized as follows. The three-mode coupled optomechanical system model and the system dynamics are described in Sec. II. The steady-state thermophonon flux is evaluated in terms of the first and second moments of the system, and the general expression of the flux is derived by the cumulant generating function approach in Sec. III. Section IV provides a discussion of how thermophonon flux between the mechanical oscillator and the coupled system is regulated by changing the system parameters. Finally, a discussion of the general points of the study is presented in Sec. V.

II. MODEL AND SYSTEM DYNAMICS

As schematically shown in Fig. 1(a), our model is a three-mode coupled optomechanical system consisting of a passive cavity, an active cavity, and a mechanical oscillator. The main aim is to investigate the thermophonon transports from the thermal bath of the mechanical oscillator to the coupled system. Here the left cavity is passive and the decay rate and the resonance frequency of the cavity are, respectively, γ and ω_{c1}; the right cavity is a gain optical cavity and the gain rate and the resonance frequency of the cavity are, respectively, κ and ω_{c2}; the loss rate and the natural frequency of the mechanical oscillator are, respectively, γ_m and ω_m. In the optomechanical subsystem, we assume that the mechanical resonator is only coupled to the left passive optical cavity with optomechanical coupling strength g_1, where the passive cavity is driven by a strong driving field with amplitude Ω_d and frequency ω_d and injected by a squeezed vacuum field with central frequency ω_s [26,54–58]. In addition, the photon-tunneling strength between two adjacent optical cavities is J, which can be adjusted by changing the distance between adjacent cavities [59–61].

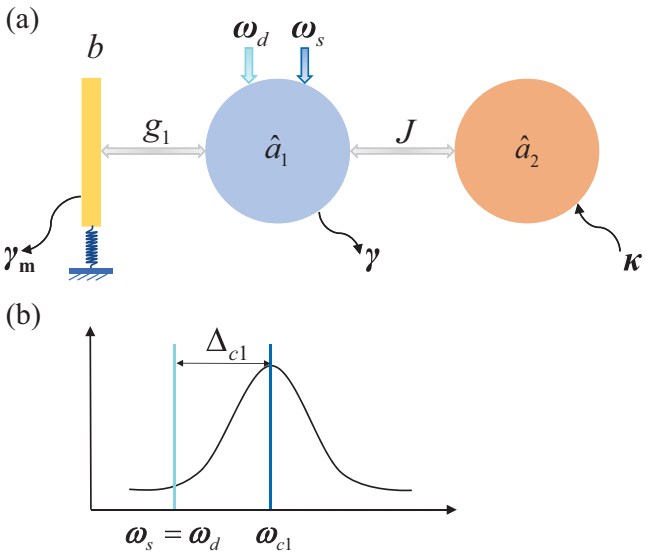

FIG. 1. (a) Schematic illustration of a three-mode coupled optomechanical system consisting of a passive cavity, an auxiliary active cavity, and a mechanical oscillator. In this setup, the quantum mechanical oscillator and the right active cavity ($\hat{a}_2$) simultaneously couple to the left passive cavity ($\hat{a}_1$), which is driven by an external laser with frequency ω_d and injected by a squeezed vacuum field with central frequency ω_s. (b) We also consider that the central frequency of the broadband squeezed vacuum field is equal to the driving frequency, i.e., $\omega_s = \omega_d$. From the point of thermodynamics, the mechanical oscillator is immersed in the thermal bath with the temperature $T > 0$ and the driven optical mode couples to the squeezed vacuum bath with an adjustable effective temperature via the squeezing parameters or photon-tunneling coupling J so that the energy transfer between the two sources can be generated and controlled by the optomechanical coupling g_1 and the cavity-pump detuning $\Delta_{c1} = \omega_{c1} - \omega_d$.

The total Hamiltonian of the system reads (setting $\hbar = 1$) [62–64]

$$H_T = \omega_{c1}\hat{a}_1^\dagger\hat{a}_1 + \omega_{c2}\hat{a}_2^\dagger\hat{a}_2 + \omega_m\hat{b}^\dagger\hat{b} - g_1\hat{a}_1^\dagger\hat{a}_1(\hat{b}^\dagger + \hat{b}) + J(\hat{a}_1^\dagger\hat{a}_2 + \hat{a}_2^\dagger\hat{a}_1) + i(\hat{a}_1^\dagger\Omega_d e^{-i\omega_d t} - \hat{a}_1\Omega_d^* e^{i\omega_d t}). \quad (1)$$

Here, $\hat{a}_1$ ($\hat{a}_1^\dagger$) and $\hat{a}_2$ ($\hat{a}_2^\dagger$) denote the annihilation (creation) operators of the passive and the active cavities, respectively; $\hat{b}$ ($\hat{b}^\dagger$) is the annihilation (creation) operator of the mechanical oscillator. The single-photon optomechanical coupling g_1 between the passive cavity and the mechanical oscillator can be expressed as $g_1 = (\omega_{c1}/L_0)\sqrt{\hbar/(2m\omega_m)}$, where the cavity length and the mass of the mechanical oscillator are, respectively, L_0 and m. The amplitude of the input field can be normalized to the photon flux, i.e., $\Omega_d = \sqrt{2P\gamma/(\hbar\omega_d)}$, in terms of the power of the laser P and the cavity length L_0. Further, considering the rotating-wave approximation of the system and combining the transformation $H \to U^\dagger H_T U - iU^\dagger\partial_t U$ written into the interaction picture with respect to $U = \exp[-i\omega_d(\hat{a}_1^\dagger\hat{a}_1 + \hat{a}_2^\dagger\hat{a}_2)t]$, the total Hamiltonian of the

system becomes

$$H = \Delta_{c1}\hat{a}_1^\dagger\hat{a}_1 + \Delta_{c2}\hat{a}_2^\dagger\hat{a}_2 + \omega_m\hat{b}^\dagger\hat{b} - g_1\hat{a}_1^\dagger\hat{a}_1(b^\dagger + \hat{b}) + J(\hat{a}_1^\dagger\hat{a}_2 + \hat{a}_2^\dagger\hat{a}_1) + i(\hat{a}_1^\dagger\Omega_d - \hat{a}_1\Omega_d^*), \quad (2)$$

where $\Delta_{ci} = \omega_{ci} - \omega_d$ $(i = 1, 2)$ denotes the cavity-pump detuning between the cavity field i and the driving field.

The quantum dynamics of the coupled optomechanical system can be investigated using the Heisenberg-Langevin equation with Hamiltonian (2). It is noted that in addition to the evolution described by the Hamiltonian, the full dynamics of the system should include the fluctuation-dissipation processes affecting the optical fields and mechanical oscillators. Using the Hamiltonian (2) and taking into account the quantum fluctuations, the dynamics of the system can be described by the following quantum Langevin equations (QLEs):

$$\dot{\hat{a}}_1 = -i\Delta_{c1}\hat{a}_1 + ig_1\hat{a}_1(\hat{b} + \hat{b}^\dagger) - iJ\hat{a}_2 + \Omega_d - \gamma\hat{a}_1 + \sqrt{2\gamma}\hat{a}_{1,\mathrm{in}}(t), \quad (3)$$

$$\dot{\hat{a}}_2 = -i\Delta_{c2}\hat{a}_2 - iJ\hat{a}_1 + \kappa\hat{a}_2 + \sqrt{2\kappa}\hat{a}_{2,in}(t), \quad (4)$$

$$\dot{\hat{b}} = -i\omega_m\hat{b} + ig_1\hat{a}_1^\dagger\hat{a}_1 - \gamma_m\hat{b} + \sqrt{2\gamma_m}\hat{b}_{\mathrm{in}}(t), \quad (5)$$

where $\hat{a}_{1,in}$ and $\hat{a}_{2,in}$ denote the input noise operators acting on the cavity modes, and $\hat{b}_{\mathrm{in}}$ is the thermal noise operator acting on the mechanical oscillator. Here we consider that the injected vacuum noise of the passive cavity is squeezed, which can usually be provided by a finite bandwidth output of an optical parametric oscillator (OPO). This means that the driven cavity mode is subject to a non-Markovian squeezed vacuum noise and the corresponding correlation functions will significantly depend on the bandwidth properties of the injected squeezing light field [26]. However, in the white-noise limit for squeezing, the cavity is driven by a broadband squeezed vacuum field and therefore the quantum vacuum fluctuations of the passive cavity field satisfy the nonzero time-domain correlation functions [26,56,57],

$$\langle\hat{a}_{1,\mathrm{in}}(t)\hat{a}_{1,\mathrm{in}}(t')\rangle = M_s e^{-i(\omega_s-\omega_d)(t+t')}\delta(t-t'), \quad (6)$$

$$\langle\hat{a}_{1,in}^\dagger(t)\hat{a}_{1,in}(t')\rangle = N_s\delta(t-t'), \quad (7)$$

$$\langle\hat{a}_{1,\mathrm{in}}(t)\hat{a}_{1,\mathrm{in}}^\dagger(t')\rangle = (N_s+1)\delta(t-t'), \quad (8)$$

where M_s and N_s denote two control parameters related to the squeezed vacuum injection. In particular, in the case of pure squeezing, $M_s = (1/2)\sinh(2r)e^{i\theta}$ and $N_s = \sinh^2(r)$, with r and θ being the strength and the phase of squeezing, respectively. Further, we consider that the central frequency of the broadband squeezed vacuum field is equal to the driving frequency, i.e., $\omega_s = \omega_d$ [see Fig. 1(b)]. In this case, the first correlation of the quantum vacuum fluctuation [Eq. (6)] can be simplified as [58]

$$\langle\hat{a}_{1,\mathrm{in}}(t)\hat{a}_{1,\mathrm{in}}(t')\rangle = M_s\delta(t-t'). \quad (9)$$

For the active cavity with gain, the quantum vacuum fluctuation of the cavity field is assumed to be δ correlated [50,65],

$$\langle\hat{a}_{2,\mathrm{in}}^\dagger(t)\hat{a}_{2,\mathrm{in}}(t')\rangle = \delta(t-t'), \quad (10)$$

$$\langle\hat{a}_{2,\mathrm{in}}(t)\hat{a}_{2,\mathrm{in}}^\dagger(t')\rangle = 0. \quad (11)$$

In addition, the nonzero correlation functions for the thermal noise are as follows [50,66]:

$$\langle\hat{b}_{\mathrm{in}}(t)\hat{b}_{\mathrm{in}}^\dagger(t')\rangle = (n_t+1)\delta(t-t'), \quad (12)$$

$$\langle\hat{b}_{\mathrm{in}}^\dagger(t)\hat{b}_{\mathrm{in}}(t')\rangle = n_t\delta(t-t'), \quad (13)$$

where n_t is the mean thermal phonon number of the mechanical mode, defined by $n_t = 1/[\exp(\hbar\omega_m/k_BT) - 1]$, with k_B and T being the Boltzmann constant and the environmental temperature, respectively.

Next we derive the linearized dynamics of the quantum fluctuations around the steady-state expectation values of the coupled system. This can be achieved by rewriting each Heisenberg operator as a c-number steady-state value plus an additional fluctuation operator with zero-mean value, i.e., $\hat{O} = O_s + \delta\hat{O}$ $(O = a_1, a_2, b)$. Then, by inserting this ansatz into Eqs. (3)–(5) and neglecting all the higher-order terms of δO, the steady-state expectation values of the coupled optomechanical system are as follows:

$$a_{1s} = \frac{(\kappa - i\Delta_{c2})\Omega_d}{(\kappa - i\Delta_{c2})(\gamma + i\Delta) - J^2}, \quad (14)$$

$$a_{2s} = \frac{iJ\Omega_d}{(\kappa - i\Delta_{c2})(\gamma + i\Delta) - J^2}, \quad (15)$$

$$b_s = \frac{ig_1|a_{1s}|^2}{\gamma_m + i\omega_m}, \quad (16)$$

where $\Delta = \Delta_{c1} - 2g_1b_s$ is the effective cavity detuning. The corresponding evolution of the quantum fluctuations is obtained as

$$\delta\dot{\hat{b}} = (-i\omega_m - \gamma_m)\delta\hat{b} + ig_1\hat{a}_{1s}(\delta\hat{a}_1 + \delta\hat{a}_1^\dagger) + \sqrt{2\gamma_m}\hat{b}_{\mathrm{in}}(t), \quad (17)$$

$$\delta\dot{\hat{a}}_1 = (-i\Delta - \gamma)\delta\hat{a}_1 + ig_1\hat{a}_{1s}(\delta\hat{b}^\dagger + \delta\hat{b}) - iJ\delta\hat{a}_2 + \sqrt{2\gamma}\hat{a}_{1,\mathrm{in}}(t), \quad (18)$$

$$\delta\dot{\hat{a}}_2 = (-i\Delta_{c2} + \kappa)\delta\hat{a}_2 - iJ\delta\hat{a}_1 + \sqrt{2\kappa}\hat{a}_{2,\mathrm{in}}(t). \quad (19)$$

In order to solve the operator equations (17)–(19) and derive their second moments determining the heat flux, we adopt a semiclassical method by converting these operator equations to a set of c-number Langevin equations [55],

$$\dot{B} = (-i\omega_m - \gamma_m)B + ig_1a_{1s}(A_1 + A_1^*) + F_B(t), \quad (20)$$

$$\dot{A}_1 = (-i\Delta - \gamma)A_1 + ig_1a_{1s}(B^* + B) - iJA_2 + F_{A_1}(t), \quad (21)$$

$$\dot{A}_2 = (\kappa - i\Delta_{c2})A_2 - iJA_1 + F_{A_2}(t), \quad (22)$$

where c-number variables A_i and B are, respectively, related to the fluctuations of the field i and the mechanical oscillator. It is noted that in the derivation of Eqs. (20)–(22), we have chosen the antinormal ordering of operators, i.e., $\delta\hat{b}$, $\delta\hat{a}_1$, $\delta\hat{a}_2$, $\delta\hat{b}^\dagger$, $\delta\hat{a}_1^\dagger$, $\delta\hat{a}_2^\dagger$, such that their first and second moments are always identical with Eqs. (17)–(19). Furthermore, the functions F_B, F_{A1}, and F_{A2} in Eqs. (20)–(22) are again the typical Langevin noise forces which obey $\langle F_k(t)\rangle = 0$ and $\langle F_k(t)F_l(t')\rangle = \langle 2D_{kl}\rangle\delta(t-t')$, where F_k and F_l can be any of the above noise forces. The diffusion coefficients D_{kl} should be determined by the requirement that

the evolution equations for the second moments are always identical to the corresponding operator equations. This leads to that some of the diffusion coefficients will be altered when the operator equations (17)–(19) are converted to the c-number equations (20)–(22). As an example, we derive the diffusion coefficient D_{BA_1}. From the operator equations (17) and (18), the time evolution of the second moment $\langle\delta\hat{b}\delta\hat{a}_1\rangle$ is [55]

$$\frac{d}{dt}\langle\delta\hat{b}\delta\hat{a}_1\rangle = [-i(\omega_m+\Delta)-\gamma_m-\gamma]\langle\delta\hat{b}\delta\hat{a}_1\rangle + ig_1a_{1s}\langle(\delta\hat{a}_1+\delta\hat{a}_1^\dagger)\delta\hat{a}_1\rangle - iJ\langle\delta\hat{b}\delta\hat{a}_2\rangle + ig_1a_{1s}\langle\delta\hat{b}(\delta\hat{b}+\delta\hat{b}^\dagger)\rangle. \tag{23}$$

We note that the term related to $\delta\hat{a}_1^\dagger\delta\hat{a}_1$ is not our chosen order because the operator $\delta\hat{a}_1^\dagger$ is to the left of $\delta\hat{a}_1$. Therefore, we have to use the commutation relation $[\delta\hat{a}_1,\delta\hat{a}_1^\dagger]=1$ to bring this term into chosen order. Then, we obtain

$$\frac{d}{dt}\langle\delta\hat{b}\delta\hat{a}_1\rangle = [-i(\omega_m+\Delta)-\gamma_m-\gamma]\langle\delta\hat{b}\delta\hat{a}_1\rangle + ig_1a_{1s}\langle\delta\hat{a}_1(\delta\hat{a}_1+\delta\hat{a}_1^\dagger)\rangle - ig_1a_{1s} - iJ\langle\delta\hat{b}\delta\hat{a}_2\rangle + ig_1a_{1s}\langle\delta\hat{b}(\delta\hat{b}+\delta\hat{b}^\dagger)\rangle. \tag{24}$$

Further, using Eqs. (20) and (21), we obtain the corresponding c-number evolution equation,

$$\frac{d}{dt}\langle BA_1\rangle = [-i(\omega_m+\Delta)-\gamma_m-\gamma]\langle BA_1\rangle + ig_1a_{1s}\langle A_1(A_1+A_1^*)\rangle - iJ\langle BA_2\rangle + ig_1a_{1s}\langle B(B+B^*)\rangle + 2\langle F_B(t)F_{A_1}(t)\rangle. \tag{25}$$

The time evolutions of the second moments $\langle\delta\hat{b}\delta\hat{a}_1\rangle$ and $\langle BA_1\rangle$ should be equal so that the diffusion coefficient D_{BA_1} is given by

$$2D_{BA_1} = -ig_1a_{1s}/2. \tag{26}$$

Other nonvanishing c-number diffusion coefficients can be calculated in an analogous way and are given by

$$2D_{BB^*} = 2\gamma_m(n_t+1), \tag{27}$$

$$2D_{A_1A_1} = 2\gamma M_s, \tag{28}$$

$$2D_{A_1A_1^*} = 2\gamma(N_s+1). \tag{29}$$

For the convenience of calculation, we define the dimensionless amplitude and phase fluctuations of the cavity fields 1 and 2 as $X_1=\frac{A_1+A_1^*}{\sqrt{2}}$, $Y_1=\frac{A_1-A_1^*}{\sqrt{2}i}$, $X_2=\frac{A_2+A_2^*}{\sqrt{2}}$, and $Y_2=\frac{A_2-A_2^*}{\sqrt{2}i}$. The corresponding noise functions are, respectively, $F_{x_1}(t)=\frac{F_{A_1}+F_{A_1}^*}{\sqrt{2}}$, $F_{y_1}(t)=\frac{F_{A_1}-F_{A_1}^*}{\sqrt{2}i}$, $F_{x_2}(t)=\frac{F_{A_2}+F_{A_2}^*}{\sqrt{2}}$, and $F_{y_2}(t)=\frac{F_{A_2}-F_{A_2}^*}{\sqrt{2}i}$. Similarly, $q=\frac{B+B^*}{\sqrt{2}}$ and $p=\frac{B-B^*}{\sqrt{2}i}$ are, respectively, the position and momentum fluctuations of the mechanical oscillator; $\xi_q(t)=\frac{F_B+F_B^*}{\sqrt{2}}$ and $\xi_p(t)=\frac{F_B-F_B^*}{\sqrt{2}i}$ are the noises related to the position and momentum. Then, the linearized c-number Langevin equations can be written as

$$\dot{q} = \omega_m p-\gamma_m q+\xi_q(t), \tag{30}$$

$$\dot{X}_1 = \Delta Y_1-\gamma X_1+JY_2+F_{x_1}(t), \tag{31}$$

$$\dot{X}_2 = \kappa X_2+\Delta_{c2}Y_2+JY_1+F_{x_2}(t), \tag{32}$$

$$\dot{p} = -\omega_m q-\gamma_m p+2g_1a_{1s}X_1+\xi_p(t), \tag{33}$$

$$\dot{Y}_1 = -\Delta X_1-\gamma Y_1+2g_1a_{1s}q-JX_2+F_{y_1}(t), \tag{34}$$

$$\dot{Y}_2 = -\Delta_{c2}X_2+\kappa Y_2-JX_1+F_{y_2}(t). \tag{35}$$

Using Eqs. (26)–(35), we can obtain the nonzero c-number correlation functions for the thermal and vacuum noises as

$$\langle\xi_q(t)\xi_q(t')\rangle = 2\gamma_m(n_t+1)\delta(t-t'), \tag{36}$$

$$\langle\xi_p(t)\xi_p(t')\rangle = 2\gamma_m(n_t+1)\delta(t-t'), \tag{37}$$

$$\langle F_{x_1}(t)F_{x_1}(t')\rangle = 2\gamma n_+\delta(t-t'), \tag{38}$$

$$\langle F_{y_1}(t)F_{y_1}(t')\rangle = 2\gamma n_-\delta(t-t'), \tag{39}$$

$$\langle F_{x_1}(t)\xi_p(t')\rangle = -g_1a_{1s}/2\delta(t-t'), \tag{40}$$

$$\langle\xi_q(t)F_{y_1}(t')\rangle = -g_1a_{1s}/2\delta(t-t'), \tag{41}$$

$$\langle F_{x_1}(t)F_{y_1}(t')\rangle = 2\gamma M_s^I\delta(t-t'), \tag{42}$$

where $n_\pm = N_s+1\pm M_s^R$ with $M_s^R=\frac{(M_s+M_s^*)}{2}$ and $M_s^I=\frac{(M_s-M_s^*)}{2i}$. Further, Eqs. (30)–(35) can be written in the matrix form,

$$\dot{x} = -K_1x+\Phi_1y+f_x(t), \tag{43}$$

$$\dot{y} = -K_1y-\Phi_2x+f_y(t), \tag{44}$$

where x, y, $f_x(t)$, and $f_y(t)$ are the column vector. Their transposes are, $x^T=(q,X_1,X_2)$, $y^T=(p,Y_1,Y_2)$, $f_x(t)^T=[\xi_q(t),F_{x_1}(t),F_{x_2}(t)]$, and $f_y(t)^T=[\xi_p(t),F_{y_1}(t),F_{y_2}(t)]$, respectively; the matrices K_1, Φ_1, and Φ_2 are, respectively, given by

$$K_1 = \begin{pmatrix}\gamma_m & 0 & 0\\ 0 & \gamma & 0\\ 0 & 0 & -\kappa\end{pmatrix}, \tag{45}$$

$$\Phi_1 = \begin{pmatrix}\omega_m & 0 & 0\\ 0 & \Delta & J\\ 0 & J & \Delta_{c2}\end{pmatrix}, \tag{46}$$

$$\Phi_2 = \begin{pmatrix}\omega_m & -2g_1a_{1s} & 0\\ -2g_1a_{1s} & \Delta & J\\ 0 & J & \Delta_{c2}\end{pmatrix}. \tag{47}$$

III. STEADY-STATE THERMOPHONON FLUX

We focus on the study of the thermophonon transports between the thermal bath and the squeezed vacuum bath.

This can be evaluated by calculating the steady-state average thermophonon flux flowing from the thermal bath into the system in a given time duration τ, defined as

$$J_p = \lim_{\tau\to\infty} \langle \hat{N}_{p0}(\tau)\rangle/\tau, \tag{48}$$

where $\hat{N}_{p0}(\tau)$ is the number of the thermophonons induced by the noise acting on the momentum of the mechanical oscillator and can be expressed as [67–69]

$$\hat{N}_{p0}(\tau) = \int_0^\tau [\hat{\xi}_p(t) - \gamma_m \hat{p}(t)]\hat{p}(t)dt, \tag{49}$$

with $\hat{\xi}_p(t) = i(\hat{b}^{\text{in},\dagger} - \hat{b}^{\text{in}})/\sqrt{2}$ and $\hat{p} = i(\hat{b}^\dagger - \hat{b})/\sqrt{2}$ being the thermal noise and the momentum of the oscillator. Clearly, it is seen from Eq. (49) that the average of the thermophonon number is determined by the first and second moments of Eqs. (17)–(19). Using the ansatz $\hat{O} = O_s + \delta\hat{O}$, the thermophonon number can be written as

$$\hat{N}_{p0}(\tau) = -\gamma_m p_s^2 \tau + \int_0^\tau [\hat{\xi}_p(t) - \gamma_m \delta\hat{p}(t)]\delta\hat{p}(t)dt, \tag{50}$$

in terms of the steady-state value of momentum $p_s = (b_s - b_s^*)/(\sqrt{2}i)$ and its fluctuation $\delta\hat{p} = (\delta\hat{b} - \delta\hat{b}^\dagger)/(\sqrt{2}i)$. The second term in Eq. (50) is a fluctuating quantity and its average is the same as that of the particle number, $N_p(\tau) = \int_0^\tau [\xi_p(t) - \gamma_m p(t)]p(t)dt$, defined by the c-number quadrature $p(t)$ in Eqs. (43) and (44), which depends on the initial conditions of the system and the noise trajectory in any particular realization. In order to evaluate the average of N_p, we introduce the probability distribution of N_p, $\mathcal{P}(N_p, \tau)$ and the characteristic function for the thermophonon counting field λ, $Z(\lambda) = \langle e^{-\lambda N_p}\rangle$, averaging initial configurations and different paths [70,71]. In general, for the given initial and final configurations U_0 and U in time τ with $U^T = (x^T, y^T)$, the characteristic function $Z(\lambda, U, \tau|U_0)$ satisfies a Fokker-Planck (FP) type of equation [70],

$$[\partial_\tau - L_\lambda]Z(\lambda, U, \tau|U_0) = 0, \tag{51}$$

where $Z(\lambda, U, \tau|U_0) = \langle e^{-\lambda N_p}\rangle_{U_0,U}$ and the initial condition $Z(\lambda, U, \tau|U_0) = \delta(U - U_0)$; L_λ is the FP operator related to Eqs. (43) and (44), whose specific forms are not necessary [69]. This is because we are interested in the restricted characteristic function in the large-τ limit and the steady-state distribution, which is only determined by the largest eigenvalue $\mu(\lambda)$ of the operator $L(\lambda)$, i.e., $Z(\lambda, \tau) \approx e^{\tau\mu(\lambda)}$ [70], and is difficult to attain by directly solving the FP equation. In spite of this fact, by using the finite-time Fourier transforms of Eqs. (43) and (44) and the Gaussian distribution characteristics of thermal and vacuum noises, the largest eigenvalue can be still evaluated as [70,71]

$$\mu(\lambda) = -\frac{1}{4\pi}\int_{-\infty}^{\infty} d\omega \ln[\det(I + 2\gamma_m\lambda\tau D\Upsilon_n)], \tag{52}$$

where D is the 6×6 noise matrix,

$$D = \frac{1}{\tau}\begin{pmatrix} 2\gamma_m\bar{n} & 0 & 0 & 0 & -\frac{g_1 a_{1s}}{2} & 0 \\ 0 & 2\gamma n_+ & 0 & -\frac{g_1 a_{1s}}{2} & 2\gamma M_s^I & 0 \\ 0 & 0 & 0 & 0 & 0 & 0 \\ 0 & -\frac{g_1 a_{1s}}{2} & 0 & 2\gamma_m\bar{n} & 0 & 0 \\ -\frac{g_1 a_{1s}}{2} & 2\gamma M_s^I & 0 & 0 & 2\gamma n_- & 0 \\ 0 & 0 & 0 & 0 & 0 & 0 \end{pmatrix}, \tag{53}$$

with $\bar{n} = n_t + 1$, and Υ_n is the coefficient matrix related to the coefficients of Eqs. (43) and (44), i.e.,

$$\Upsilon_n(\omega) = \begin{pmatrix} -|N_{11}|^2 & -N_{11}N_{12}^* & -N_{11}N_{13}^* & N_{11}\Upsilon_{11}^* & N_{11}M_{12}^* & N_{11}M_{13}^* \\ -N_{11}^*N_{12} & -|N_{12}|^2 & -N_{12}N_{13}^* & N_{12}\Upsilon_{11}^* & N_{12}M_{12}^* & N_{12}M_{13}^* \\ -N_{11}^*N_{13} & -N_{12}^*N_{13} & -|N_{13}|^2 & N_{13}\Upsilon_{11}^* & N_{13}M_{12}^* & N_{13}M_{13}^* \\ N_{11}^*\Upsilon_{11} & N_{12}^*\Upsilon_{11} & N_{13}^*\Upsilon_{11} & \frac{M_{11}^*}{(2\gamma_m)} - M_{11}\Upsilon_{11}^* & -M_{12}^*\Upsilon_{11} & -M_{13}^*\Upsilon_{11} \\ N_{11}^*M_{12} & N_{12}^*M_{12} & N_{13}^*M_{12} & -M_{12}\Upsilon_{11}^* & -|M_{12}|^2 & -M_{12}M_{13}^* \\ N_{11}^*M_{13} & N_{12}^*M_{13} & N_{13}^*M_{13} & -M_{13}\Upsilon_{11}^* & M_{12}^*M_{13} & -|M_{13}|^2 \end{pmatrix}, \tag{54}$$

where $\Upsilon_{11} = M_{11} - 1/(2\gamma_m)$, $M(\omega) = (K_2)^{-1}(I - \Phi_2 A\Phi_1)$, $N(\omega) = (K_2)^{-1}\Phi_2 A K_2$, with $K_2(\omega) = K_1 + I\times i\omega$ and $A(\omega) = [(K_2)^2 + \Phi_1\Phi_2]^{-1}$; N_{ij} with $i, j = 1, 2, 3$ denotes the element of the ith row and the jth column of matrix N and so on.

In particular, the eigenvalue $\mu(\lambda)$ can be used to describe the cumulant generating function (CGF) of the coupled oscillator system, which is given by $\mathcal{G}(\lambda) = \lim_{\tau\to\infty} \ln Z(\lambda)/\tau$ and contains information about the first-order cumulant of thermophonon current fluctuations, such as $J_1(\tau) = \lim_{\tau\to\infty}\langle N_p\rangle/\tau = -\partial G(\lambda)/\partial\lambda|_{\lambda=0}$ [5,70]. Consequently, the total average thermophonon flux $J_p = \lim_{\tau\to\infty}\langle N_{p0}(\tau)\rangle/\tau$ becomes

$$J_p = -\gamma_m p_s^2 - \partial_\lambda \mu(\lambda)|_{\lambda=0}. \tag{55}$$

Finally, the steady-state thermophonon flow is

$$J_p = -\gamma_m p_s^2 + \frac{1}{4\pi}\int_{-\infty}^{\infty} d\omega\{\text{Tr}[2\gamma_m D\tau\Upsilon_n(\omega)]\}. \tag{56}$$

IV. RESULTS AND DISCUSSIONS

We now numerically evaluate the values of the steady-state thermophonon flux with experimentally accessible parameters and study the effect of the optical parameters on the flux in the three-mode optomechanical system. In particular, we are also interested in the reversion of the thermophonon flux by controlling the gain of the active cavity and the squeezed strength r. In order to achieve this goal, we consider that the system works in the regime of the weak optomechanical coupling, i.e., $g_1 = 7.4\times 10^{-5}\gamma$ with $\gamma = 2\pi$ MHz being the decay

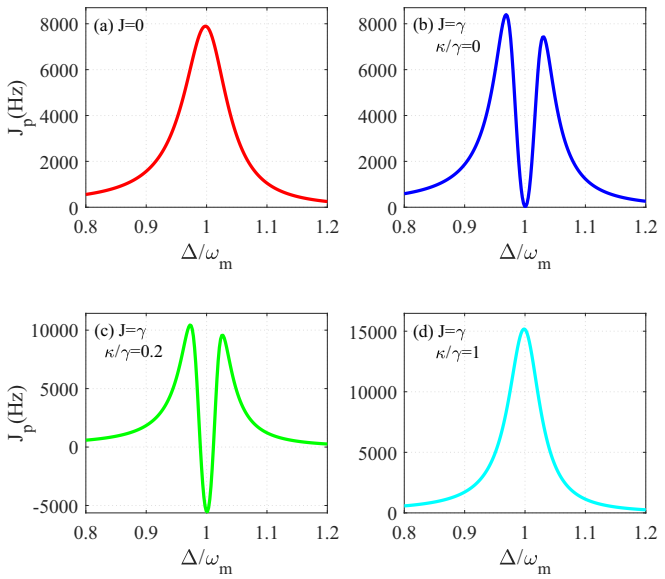

FIG. 2. The thermophonon fluxes J_p are plotted as a function of the normalized detuning δ/ω_m for different values of J and κ/γ. (a) The case of a single optical cavity with $J = 0$. (b)–(d) The cases of two coupled optical cavities ($J = \gamma$ and $\Delta_{c2} = \Delta$) with κ/γ being 0, 0.2, and 1, respectively. The other parameter values we selected are $\lambda_d = 1550$ nm, $L = 1$ mm, $m = 50$ ng, $\omega_m = 2\pi \times 23$ MHz, $\gamma = 2\pi$ MHz, $\gamma_m = 1.63 \times 10^{-3}\gamma$, $g_1 = 7.4 \times 10^{-5}\gamma$, and $r = 0$.

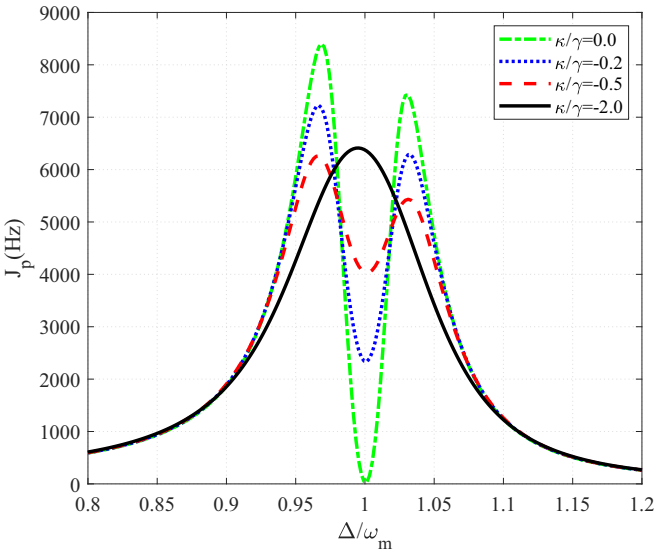

FIG. 3. The thermophonon fluxes J_p are plotted as a function of the normalized detuning Δ/ω_m with different values of the loss rate κ when the coupled cavity is also passive. The coupling strength J is fixed as $J = \gamma$ and the other parameter values are the same as in Fig. 2.

rate of the left passive cavity. The mechanical oscillation frequency is $\omega_m = 2\pi \times 23$ MHz, the damping rate is $\gamma_m = 1.63 \times 10^{-3}\gamma$, and the mass is $m = 50$ ng. The wavelength and the power of the driving field are, respectively, $\lambda_d = 1550$ nm and $P = 0.001$ mW. The length of the cavity is $L = 1$ mm. In Fig. 2, we show the steady-state thermophonon flux J_p as a function of the normalized detuning Δ/ω_m in the case of a single optical cavity with $J = 0$ [Fig. 2(a)], and the case of two coupled optical cavities ($J = \gamma$ and $\Delta_{c2} = \Delta$) with different κ/γ's [Figs. 2(b)–2(d)]. In the numerical result, we also temporarily remove the squeezed vacuum injection with $r = 0$. It is clear from Fig. 2(a) that for a typical two-mode optomechanical system, the steady-state flux J_p is not a monotonous function of the effective detuning and its maximum appears at an optimal effective detuning, i.e., $\Delta = \omega_m$. This is because in the case of $\Delta \approx \omega_m$, the beam-splitter interaction between the mechanical mode and the optical field, i.e., $\delta\hat{a}_1^\dagger\delta\hat{b} + \delta\hat{a}_1\delta\hat{b}^\dagger$ in the effective Hamiltonian corresponding to Eqs. (17)–(19), is in resonance and therefore the cooling process of the mechanical oscillator dominates the system dynamics, which is mediated by the quantum transitions between the states of the system on the energy scale of the mechanical quantum and corresponds to the most efficient energy transfer from the mechanical oscillator to the optical mode.

When an additional optical cavity without the gain and loss is coupled to the passive cavity, i.e., $J = \gamma$ and $\kappa/\gamma = 0$ in Fig. 2(b), the dependence of the flux on the effective detuning is changed significantly. For example, we can see from Fig. 2(b) that the peak of the flux is split and therefore there always exists a dip in thermophonon transport which is obtained as $\Delta = \omega_m$. That is, in the presence of the coupled cavity, the flux profile at $\Delta = \omega_m$ reverses from the peak to the dip. Physically, this originates from the increase of the interference channels between the states, in contrast to the case with only optomechanical coupling, which can suppress the cooling process of the mechanical oscillator and therefore weaken the energy exchange from the thermal bath to the vacuum one. In particular, when the coupled cavity is a gain cavity, i.e., $\kappa/\gamma = 0.2$, from Fig. 2(c) we find that the dip becomes negative so that the energy transport from the coupled system to the thermal bath becomes possible. This means that in this case, the heating effect of the mechanical oscillator will exceed its cooling one when the heating process of the mechanical oscillator dominates the system dynamics. In general, when a gain system is coupled to the passive cavity, the energy is driven to flow from the coupled system with gain to the dissipation thermal environment. However, when the gain of the coupled cavity increases further, i.e., the case of the balanced gain and loss with $\kappa/\gamma = 1$, we see from Fig. 2(d) that the flux profile with a single peak reappears and the steady-state flux always flows from the thermal bath to the coupled system. Furthermore, from Figs. 2(a) and 2(d), we can see that the maximum of the steady-state flux in the case of the balanced gain and loss is much larger than that of the case with only optomechanical coupling and therefore the additional gain cavity can drive the thermal energy to be exchanged more quickly due to the field localization effect in the gain cavity [25]. We stress that the present coupled system works in the $\mathcal{PT}$-symmetric phase and therefore is always stable. These results indicate that the noise current value and its direction in the optomechanical system can be maneuvered by coupling a mechanical oscillator to the dimer system with a gain cavity.

We can study the effect of κ/γ on the thermophonon flux by considering that the additionally coupled cavity is passive, i.e., $\kappa/\gamma < 0$. In Fig. 3, we show the steady-state flux J_p as

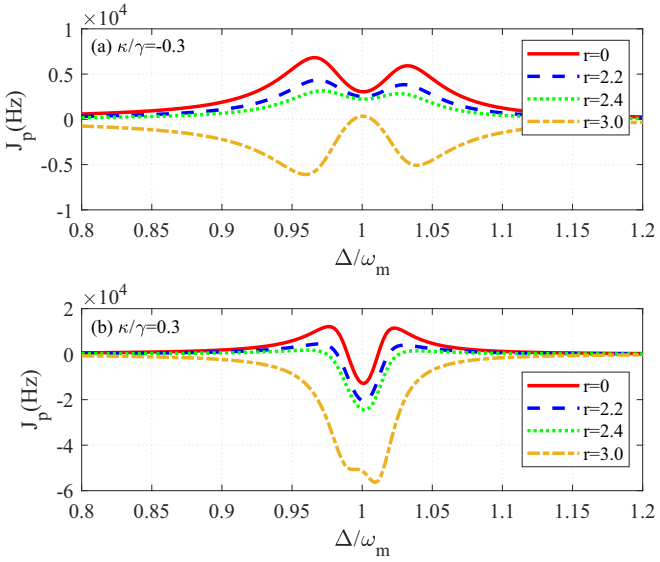

FIG. 4. The thermophonon fluxes J_p are plotted as a function of the normalized detuning Δ/ω_m with different values of the squeezed strength r for the case of the (a) passive-passive cavity and (b) passive-active cavity. The coupling strength $J = \gamma$, the squeezed phase $\theta = \pi/2$, and the other parameter values are the same as in Fig. 2.

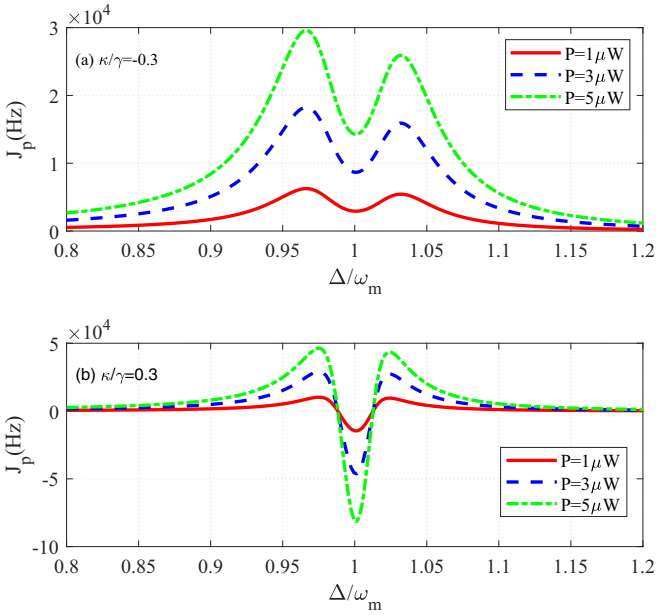

FIG. 5. The thermophonon fluxes J_p are plotted as a function of the normalized detuning Δ/ω_m with different values of the driving power P for the case of the (a) passive-passive cavity and (b) passive-active cavity. The squeezed strength $r = 1.5$ and the other parameter values are the same as in Fig. 4.

a function of Δ/ω_m with different values of $\kappa/\gamma \leqslant 0$. We can see that the depth of the dip gradually becomes shallow with increasing the loss rate κ. In addition, increasing the loss always leads to the suppression of both the sideband peaks of the flux and, finally, the flux profile changes from two peaks to one. Consequently, in the resonant regime of $\Delta \approx \omega_m$, the bath of the second passive optical cavity plays a more and more important role as an additional channel of energy dissipation. In contrast, in the sideband regimes of $\Delta = \omega_m$, increasing the decay of the coupled cavity will decline the steady-state flux flowing from the thermal bath to the vacuum baths. It is noted that for the passive-passive coupled system, the steady-state fluxes are always positive with different κ's because the baths of the optical fields are dissipative so that the effective temperature of the optical mode is less than the temperature of the thermal bath.

We also discuss in detail the effect of the squeezed parameter r on the steady-state flux, as shown in Fig. 4. We fix the gain or loss of the second cavity, i.e., $\kappa/\gamma = 0.3$ [Fig. 4(a)] and $\kappa/\gamma = -0.3$ [Fig. 4(b)], and gradually change the values of the parameter r from 0 to 3. In Fig. 4(a), it is shown that when the left passive cavity is coupled to a loss cavity, increasing the values of r not only declines the peaks of the positive flux, but also increases the depth of the dip at $\Delta = \omega_m$. This is because when the squeezed parameter r increases, the increasing noise correlation enhances the effective temperature of the optical mode in the passive cavity and therefore weakens the nonequilibrium characteristics between the thermal bath and the squeezed vacuum bath, so that the steady-state flux decreases with the increasing r. In particular, when the squeezed strength r is relatively large, i.e., $r = 3$, the nonequilibrium characteristic between the thermal bath and the squeezed vacuum bath is reversed so that the steady-state flux becomes negative. In this case, the energy will flow from the squeezed vacuum bath to the mechanical thermal one, which can be seen as a result of the transfer of squeezing from light to mechanical oscillator [26]. Similarly, in Fig. 4(b), we can see that when the left passive cavity is coupled to the cavity with a small gain, i.e., $\kappa/\gamma = 0.3$, the energy flux at $\Delta = \omega_m$ always flows from the squeezed vacuum bath to the thermal one and increases with the increasing r.

In Fig. 5, we show the steady-state thermophonon flux J_p as a function of the normalized detuning Δ/ω_m with different driving power P. In Fig. 5(a), we can observe that in the case of the passive-passive coupled cavity, the steady-state flux always increases with increasing P. Clearly, the lager driving power P enhances the effective optomechanical coupling between the mechanical oscillator and the optical mode and therefore widens the channel of the energy transfer between them. As a result, the larger flux can be attained. Similarly, when the passive-active coupled cavity is considered, we can see from Fig. 5(b) that the two peaks of the flux and the depth of the central dip become gradually shallow with decreasing P. Therefore, the amplitude of the steady-state thermophonon flux between the thermal bath and the vacuum one can be easily controlled by adjusting the driving power.

Apart from the gain ratio, the squeezing strength, and the driving power, we also investigate the effect of the tunneling strength J on the flux shape of the three-mode optomechanical system. In Fig. 6, we plot the steady-state flux as a function of the normalized detuning Δ/ω_m with different tunneling strengths J. It is clearly shown that in the presence of the coupled cavity with gain [Figs. 6(a)–6(d)] and loss [Figs. 6(e)–6(h)], the peak of the flux can be split and the separation of the split peaks increases gradually with

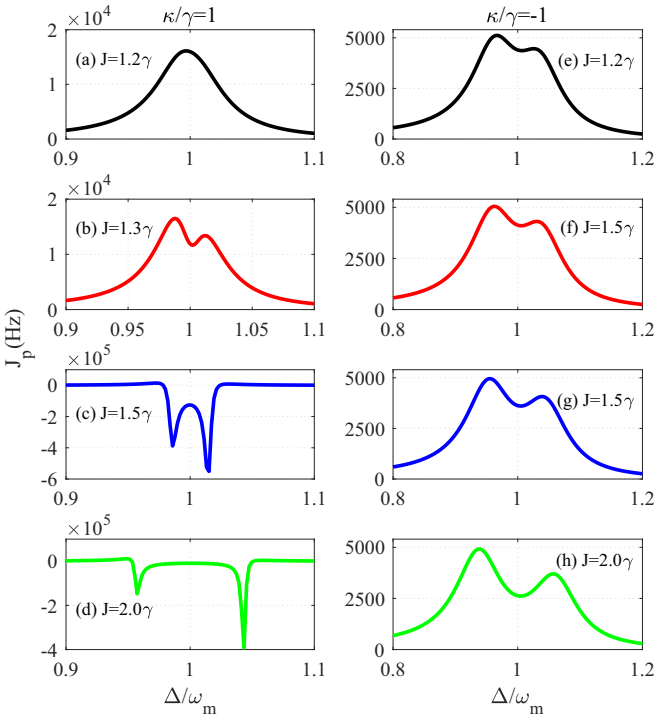

FIG. 6. The thermophonon fluxes J_p are plotted as a function of the normalized detuning Δ/ω_m with different values of the tunneling strength J for the case of the (a)–(d) passive-active cavity and (e),(f) passive-passive cavity. The squeezed strength $r = 1.5$ and the other parameter values are the same as in Fig. 4.

increasing tunneling strength J. This is because when the tunneling strength between the coupled cavity system is increased, the interference effects between the states of the coupled system are enhanced significantly, which leads to the position of the optimal flux moving outside. In particular, when the coupled cavity is active, i.e., $\kappa/\gamma = 1$, and the tunneling strengths J are large enough, i.e., $J = 1.5\gamma$, from Figs. 6(c) and 6(d), we find that the thermophonon flux can also be negative so that the energy is transferred from the coupled system to the thermal bath. We stress that the present three-mode optomechanical system with gain always works in the $\mathcal{PT}$-symmetric regime. The results suggest that the flux profile at Δ/ω_m can be conveniently modified by adjusting the tunneling strength between the adjacent optical cavities, which is easily controlled by varying the distance between the optical cavity.

V. CONCLUSIONS

In conclusion, we propose a three-mode coupled optomechanical system consisting of two coupled optical cavities and a mechanical oscillator to investigate the thermophonon transports between the coupled system and the thermal bath of the mechanical oscillator. We first derive the general expression of the steady-state thermophonon flux in the system by using the cumulant generating function approach. Then, we investigate the change of the energy transports in the three-mode system by changing the gain or loss of the coupled cavity, the strength of the squeezed vacuum, the driving power, and the tunneling strength between the adjacent cavities. It is clearly seen that due to destructive interferences among the excitation paths of two single-mode cavities, the steady-state flux profile changes from one peak to two. Further, the amplitude and direction of the steady-state flux can be flexibly controlled by changing the gain and the tunneling strength of the active cavity. In particular, the squeezed vacuum can significantly change the nonequilibrium characteristics between the thermal bath and the squeezed vacuum bath, which will reverse the thermophonon flux from positive to negative. These results present interesting transfer properties of the thermophonon in an optomechanical system coupled to dissipative environments, which provides a potential application in effectively manipulating the propagation of the thermophonon with more handles.

ACKNOWLEDGMENTS

W.J.N. is supported by the National Natural Science Foundation of China (NSFC) under Grant No. 12065008, the Key Project of Youth Science Foundation of Jiangxi Porvince under Grant No. 20192ACBL21001, and the Natural Science Foundation of Jiangxi Province under Grant No. 20192BCBL23007. A.X.C. is supported by the NSFC under Grant No. 11775190. Y.H.L. is supported by the NSFC under Grant No. 11775035.

[1] D. Segal, Phys. Rev. Lett. **101**, 260601 (2008).
[2] Y. Dubi and M. Di Ventra, Rev. Mod. Phys. **83**, 131 (2011).
[3] A. Dhar, O. Narayan, A. Kundu, and K. Saito, Phys. Rev. E **83**, 011101 (2011).
[4] N. B. Li, J. Ren, L. Wang, G. Zhang, P. Hänggi, and B. Li, Rev. Mod. Phys. **84**, 1045 (2012).
[5] J. Ren, S. Liu, and B. Li, Phys. Rev. Lett. **108**, 210603 (2012).
[6] S. Liu, B. K. Agarwalla, J. S. Wang, and B. Li, Phys. Rev. E **87**, 022122 (2013).
[7] E. Taylor and D. Segal, Phys. Rev. Lett. **114**, 220401 (2015).
[8] D. Segal and A. Nitzan, Phys. Rev. Lett. **94**, 034301 (2005).
[9] C. Wang, J. Ren, and J. Cao, Phys. Rev. A **95**, 023610 (2017).
[10] P. Kim, L. Shi, A. Majumdar, and P. L. McEuen, Phys. Rev. Lett. **87**, 215502 (2001).
[11] J. A. Johnson, A. A. Maznev, J. Cuffe, J. K. Eliason, A. J. Minnich, T. Kehoe, Clivia M. Sotomayor Torres, G. Chen, and K. A. Nelson, Phys. Rev. Lett. **110**, 025901 (2013).
[12] J. Ren, P. Hanggi, and B. Li, Phys. Rev. Lett. **104**, 170601 (2010).
[13] R. Y. Wang, R. A. Segalman, and A. Majumdar, Appl. Phys. Lett. **89**, 173113 (2006).
[14] Z. Wang, J. A. Carter, A. Lagutchev, Y. K. Koh, N.-H. Seong, D. G. Cahill, and D. D. Dlott, Science **317**, 787 (2007).
[15] B. Li, L. Wang, and G. Casati, Phys. Rev. Lett. **93**, 184301 (2004).
[16] J. Ordonez-Miranda, Y. Ezzahri, and K. Joulain, Phys. Rev. E **95**, 022128 (2017).

[17] M. Terraneo, M. Peyrard, and G. Casati, Phys. Rev. Lett. **88**, 094302 (2002).
[18] N. Yang, N. Li, L. Wang, and B. Li, Phys. Rev. B **76**, 020301(R) (2007).
[19] D. Segal, Phys. Rev. Lett. **100**, 105901 (2008).
[20] I. Wilson-Rae, N. Nooshi, W. Zwerger, and T. J. Kippenberg, Phys. Rev. Lett. **99**, 093901 (2007).
[21] F. Marquardt, J. P. Chen, A. A. Clerk, and S. M. Girvin, Phys. Rev. Lett. **99**, 093902 (2007).
[22] C. Genes, D. Vitali, P. Tombesi, S. Gigan, and M. Aspelmeyer, Phys. Rev. A **77**, 033804 (2008).
[23] Y. C. Liu, Y. F. Xiao, X. Luan, and C. W. Wong, Phys. Rev. Lett. **110**, 153606 (2013).
[24] J. Chan, T. P. Alegre, A. H. Safavi-Naeini, J. T. Hill, A. Krause, S. Groblacher, M. Aspelmeyer, and O. Painter, Nature (London) **478**, 89 (2011).
[25] Y.-L. Liu and Y.-x. Liu, Phys. Rev. A **96**, 023812 (2017).
[26] K. Jähne, C. Genes, K. Hammerer, M. Wallquist, E. S. Polzik, and P. Zoller, Phys. Rev. A **79**, 063819 (2009).
[27] D. Vitali, S. Gigan, A. Ferreira, H. R. Böhm, P. Tombesi, A. Guerreiro, V. Vedral, A. Zeilinger, and M. Aspelmeyer, Phys. Rev. Lett. **98**, 030405 (2007).
[28] M. Gao, F. Lei, C. Du, and G. Long, Sci. China Phys. Mech. Astron. **59**, 610301 (2015).
[29] A. Dalafi, M. H. Naderi, and A. Motazedifard, Phys. Rev. A **97**, 043619 (2018).
[30] C. Orzel, A. K. Tuchman, M. L. Fenselau, M. Yasuda, and M. A. Kasevich, Science **291**, 2386 (2001).
[31] X.-Y. Lü, J.-Q. Liao, L. Tian, and F. Nori, Phys. Rev. A **91**, 013834 (2015).
[32] S. Weis, R. Riviere, S. Deleglise, E. Gavartin, O. Arcizet, A. Schliesser, and T. J. Kippenberg, Science **330**, 1520 (2010).
[33] A. H. Safavi-Naeini, T. P. M. Alegre, J. Chan, M. Eichenfield, M. Winger, Q. Lin, J. T. Hill, D. E. Chang, and O. Painter, Nature (London) **472**, 69 (2011).
[34] M. Karuza, C. Biancofiore, M. Bawaj, C. Molinelli, M. Galassi, R. Natali, P. Tombesi, G. Di Giuseppe, and D. Vitali, Phys. Rev. A **88**, 013804 (2013).
[35] X. Li, W. Nie, A. Chen, and Y. Lan, Phys. Rev. A **98**, 053848 (2018).
[36] Y. Dong, F. Bariani, and P. Meystre, Phys. Rev. Lett. **115**, 223602 (2015).
[37] S. Barzanjeh, M. Aquilina, and A. Xuereb, Phys. Rev. Lett. **120**, 060601 (2018).
[38] K. Zhang, F. Bariani, and P. Meystre, Phys. Rev. Lett. **112**, 150602 (2014).
[39] K. Zhang, F. Bariani, and P. Meystre, Phys. Rev. A **90**, 023819 (2014).
[40] A. U. C. Hardal, N. Aslan, C. M. Wilson, and O. E. Mustecaplioglu, Phys. Rev. E **96**, 062120 (2017).
[41] D. Gelbwaser-Klimovsky and G. Kurizki, Sci. Rep. **5**, 7809 (2015).
[42] M. T. Naseem, A. Xuereb, and O. E. Müstecaplıoğlu, Phys. Rev. A **98**, 052123 (2018).
[43] A. Dechant, N. Kiesel, and E. Lutz, Phys. Rev. Lett. **114**, 183602 (2015).
[44] A. Xuereb, A. Imparato, and A. Dantan, New. J. Phys **17**, 055013 (2015).
[45] A. Seif, W. DeGottardi, K. Esfarjani, and M. Hafezi, Nat. Commun. **9**, 1207 (2018).
[46] X.-W. Xu, Y.-X. Liu, C.-P. Sun, and Y. Li, Phys. Rev. A **92**, 013852 (2015).
[47] W. Li, C. Li, and H. Song, Phys. Rev. A **95**, 023827 (2017).
[48] X.-Y. Lü, H. Jing, J.-Y. Ma, and Y. Wu, Phys. Rev. Lett. **114**, 253601 (2015).
[49] H. Jing, S. K. Özdemir, X.-Y. Lü, J. Zhang, L. Yang, and F. Nori, Phys. Rev. Lett. **113**, 053604 (2014).
[50] B. He, L. Yang, and M. Xiao, Phys. Rev. A **94**, 031802(R) (2016).
[51] D.-Y. Wang, C.-H. Bai, S. Liu, S. Zhang, and H.-F. Wang, Phys. Rev. A **99**, 043818 (2019).
[52] H. Jing, S. K. Özdemir, Z. Geng, J. Zhang, X.-Y. Lü, B. Peng, L. Yang, and F. Nori, Sci. Rep. **5**, 9663 (2015).
[53] W. Li, Y. Jiang, C. Li, and H. Song, Sci. Rep. **6**, 31095 (2016).
[54] A. Motazedifard, F. Bemani, M. H. Naderi, R. Roknizadeh, and D. Vitali, New. J. Phys **18**, 073040 (2016).
[55] M. O. Scully and M. S. Zubairy, *Quantum Optics* (Cambridge University Press, Cambridge, 2011).
[56] S. Huang and G. S. Agarwal, New J. Phys. **11**, 103044 (2009).
[57] M. Amazioug, B. Maroufi, and M. Daoud, Eur. Phys. J. D **74**, 54 (2020).
[58] S. Bougouffa and M. Al-Hmoud, Int. J. Theor. Phys. **59**, 1699 (2020).
[59] B. P. Hou, L. F. Wei, and S. J. Wang, Phys. Rev. A **92**, 033829 (2015).
[60] K. Totsuka, N. Kobayashi, and M. Tomita, Phys. Rev. Lett. **98**, 213904 (2007).
[61] L. F. Xue, Z. R. Gong, H. B. Zhu, and Z. H. Wang, Opt. Express **25**, 17249 (2017).
[62] X. Y. Zhang, Y. Q. Guo, P. Pei, and X. X. Yi, Phys. Rev. A **95**, 063825 (2017).
[63] X. Z. Zhang, L. Tian, and Y. Li, Phys. Rev. A **97**, 043818 (2018).
[64] C. Tchodimou, P. Djorwe, and S. G. Nana Engo, Phys. Rev. A **96**, 033856 (2017).
[65] G. S. Agarwal and K. Qu, Phys. Rev. A **85**, 031802(R) (2012).
[66] J. Li, I. M. Haghighi, N. Malossi, S. Zippilli, and D. Vitali, New J. Phys. **17**, 103037 (2015).
[67] K. Sekimoto, *Stochastic Energetics* (Springer, New York, 2010).
[68] W. Nie and Y. Lan, Phys. Rev. E **86**, 011110 (2012).
[69] W. Nie, G. Li, X. Li, A. Chen, Y. Lan, and S.-Y. Zhu, Phys. Rev. A **102**, 043512 (2020).
[70] A. Kundu, S. Sabhapandit, and A. Dhar, J. Stat. Mech: Theory E (2011) P03007.
[71] D. Gupta and S. Sabhapandit, J. Stat. Mech.: Theory E (2018) 063203.